ANIMAL MODELS OF DIABETIC COMPLICATIONS CONSORTIUM
University of Michigan (U01 DK60994)

Annual Report
2005

Eva L. Feldman, M.D., Ph.D.
Neuropathy Phenotyping Core

Principal Investigator:
Eva L. Feldman, M.D., Ph.D.
University of Michigan
Department of Neurology
4414 Kresge III, 200 Zina Pitcher Place
Ann Arbor, MI 48109-0676
Phone: (734) 763-7274 Fax: (734)763-7275
Email: efeldman@umich.edu

Table of Contents

ANIMAL MODELS OF DIABETIC COMPLICATIONS CONSORTIUM
University of Michigan (U01 DK60994)

Part A:

Principal Investigator's Summary

1. Program Accomplishments:

Our main strategy is to establish neuropathy in animals using criteria that parallel the criteria used in man. We have developed a standard operating procedures manual entitled AMDCC Neuropathy Phenotyping Manual. This manual is available on online at www.amdcc.org and outlines in detail our methodology for both initial and more advanced neuropathy phenotyping.

A mouse model of diabetic neuropathy (DN) requires the key features present in the human condition (1-4). These include 1) clinical loss of sensory function, 2) electrophysiological measures of nerve impairment, and 3) anatomical evidence of nerve fiber loss. The AMDCC Neuropathy Core established a standardized set of protocols for screening and advanced phenotyping, utilizing the clinical criteria in man. Neuropathy screening begins with an evaluation of *clinical loss of sensory function* by a quantitative assessment of thermal sensitivity in the paw and tail. These tests measure the time of withdrawal from a heat stimulus applied separately to the paw or tail. *Electrophysiological measures of nerve impairment* are considered the "gold standard" for quantitative assessment of sensory and motor nerve function. The second murine screening component is assessment of motor and sensory nerve conductions in the tail and sciatic nerve. Finally, analysis of the number of small myelinated and unmyelinated fibers in the mouse footpad lend insight into function. *Anatomical evidence of nerve fiber loss* is measured in the third screening component by assessment of intraepidermal nerve fiber (IENF) density in the footpad.

In animals where screening supports the presence of DN, advanced phenotyping is available at the request of the AMDCC investigator. This involves serial quantitation of sensation with the addition of measurements of mechanical allodynia, serial nerve conduction studies including sural nerve recordings and terminal assessment of neuron and nerve structure, and biochemical and anatomical measures of oxidative stress. Quantitative axonal counts of the sural nerve in conjunction with IENF of the footpad and thigh give an accurate representation of axonal loss. TUNEL staining of the dorsal root ganglia (DRG) indicates further neuronal injury. Biochemical and anatomical measures of oxidative stress confirm the presence of oxidative damage to the nervous system, supporting the current theory that glucose-mediated oxidative stress underlies the development of DN (5-9).

Our major achievements for 2005 are presented in Table 1. Table 1 represents animal models that have completed or are currently being phenotyped by our Core. This report will discuss each animal model. Data has been entered on the AMDCC website.

Table 1. Animal Models: Complete and Ongoing Neuropathy Phenotyping

	Tail Flick Hind Paw every 8-12 weeks	NCV Measured 12 or 16 and/or 24 weeks post-diabetes	IEFD Measured at tissue harvest	Biochemistry Measured at tissue harvest	Advanced Neuropathy Phenotyping
C57BLKS db/db	X	X	X	X	X
C57BLKS db/db ± resveratrol	X	X	NA	X	NA
GCLC +/- db/db high fat diet	X	Ongoing	Ongoing	Ongoing	NA
GLUT1 tg db/db High fat diet	X	X	Ongoing	Ongoing	Ongoing
Nestin Cre// SOD2 loxP/loxP	X	X	X	X	Ongoing
Akita STZ	X	X	Ongoing	Ongoing	Ongoing
Pdx +/+ and +/-	NA	X	X	X	X
RAGE Tg STZ	Ongoing	Ongoing	Ongoing	Ongoing	Ongoing
DbA STZ ± rosiglitazone	Ongoing (only 12 wk)	Ongoing (only 12 wk)	Ongoing	Ongoing	Ongoing

X = completed NA = not applicable

C57BLKS db/db: AMDCC data over the past 2 years have now amply demonstrated that C57Bl/6J mice are relatively resistant to developing neuropathy. Although db/db C7BL/6J mice are more susceptible to microvascular complications than the STZ C57Bl/6J animals, this model remained generally resistant to progressive nephropathy and neuropathy despite genetic modifications. In continued efforts to find the best genetically modified mouse for further neuropathy studies, we completed screening and advanced phenotyping of C57BLKS db/db mice, a genetic model of type 2 diabetes (10;11). These animals develop hyperglycemia at 8 weeks, with persistent blood glucose levels greater than 400 mg/dL (12;13). After 24 weeks of diabetes, glycated hemoglobin levels are elevated in db/db mice (Fig. 1 A). The time of withdrawal (latency) from a heat stimulus applied to the tail (tail flick) or the hind paw is increased in db/db animals, reflecting loss of thermal sensation (Fig. 1B and C). Tail distal motor latencies are increased (Fig. 1E) while tail sensory and sciatic motor conduction velocities are decreased in db/db when compared to db+ control mice (Fig. 1D and F), a pattern confirming DN.

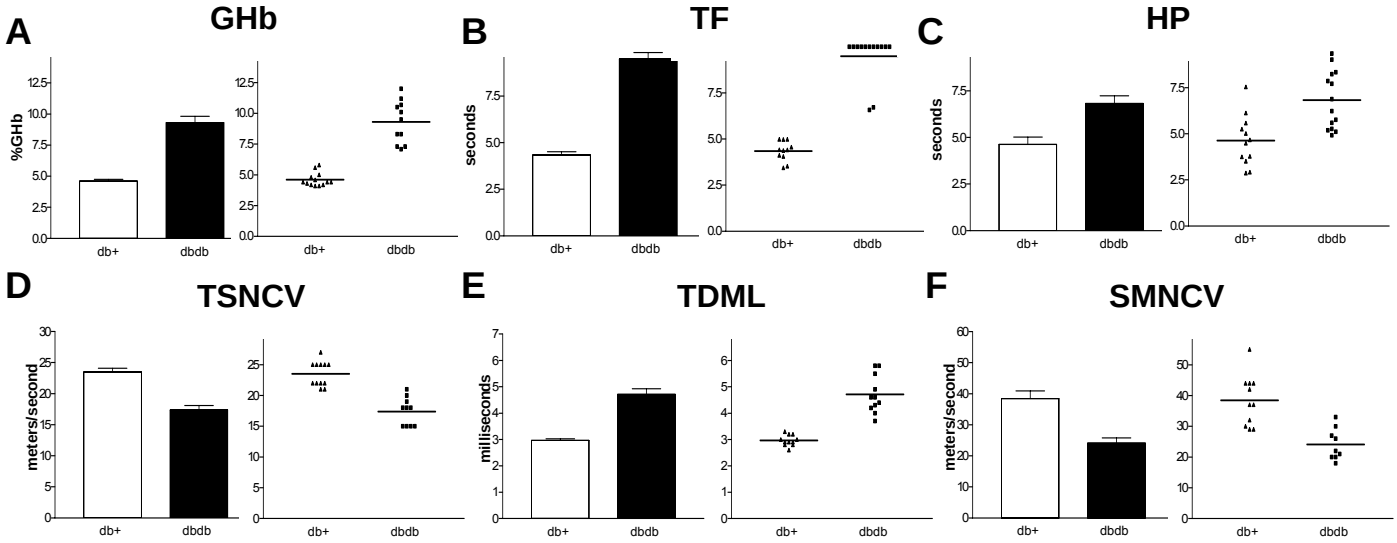

Fig. 1. Neuropathy Phenotyping Using Clinical and Electrophysiological Assessments. A full range of neuropathy phenotyping measures are used to assess nerve function in control (db+, open bars) versus diabetic (db/db, black bars) mice. In each lettered panel, the average reading ± standard error of the mean (SEM) is presented on the left and the individual animal measurements on the right. A) Db/db mice have increased glycated hemoglobin (GHb), B) Tail flick latency (TF) and C) Hind paw latencies (HP) are increased in db/db mice, D) Tail sensory nerve conduction velocity (TSNCV) is decreased in db/db mice, E) Tail distal motor latency (TDML) is increased in db/db mice, and F) Sciatic motor nerve conduction velocity (SMNCV) is decreased in db/db mice.

Anatomical evidence of nerve fiber loss in the db/db mice was measured in the third screening component by quantitative assessment of IENF in the footpad (14). The hind paws of db+ control mice are normally innervated with a full component of PGP9.5 immunoreactive fibers (Fig. 2A and C) while db/db mice have nerve fiber loss and decreased IENF (Fig. 2B and C). These differences in IENF numbers between diabetic and control mice are in agreement with published reports in human patients (14;15) and experimental rat models of DN (16).

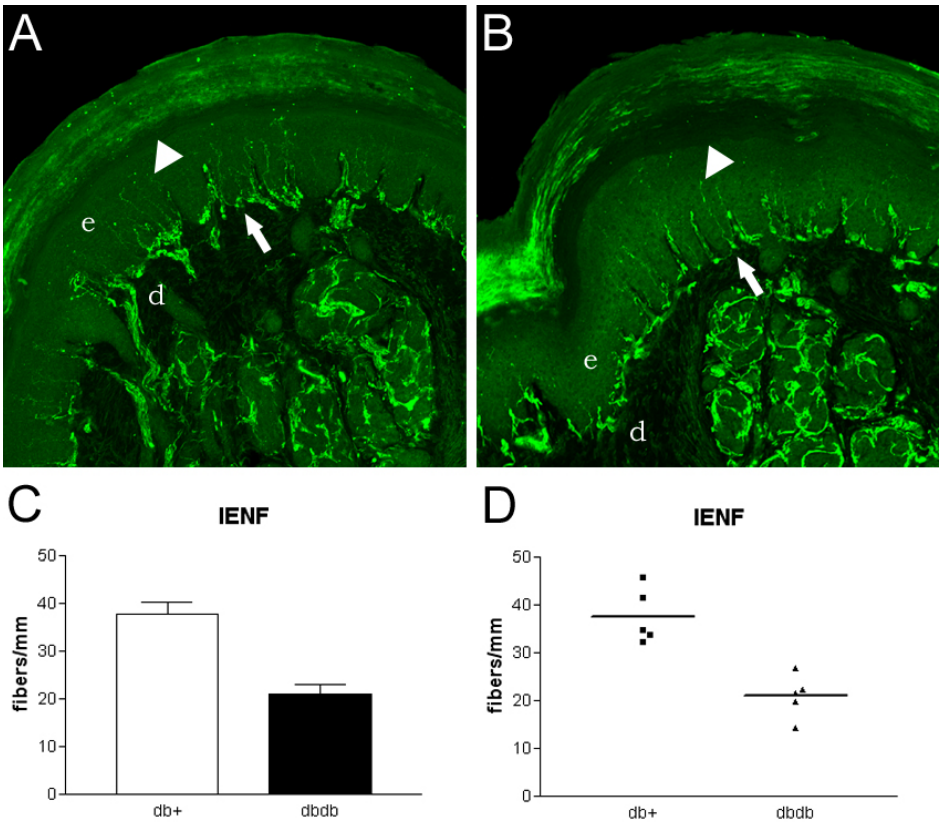

Fig. 2. Neuropathy Phenotyping Using Morphological Techniques. IENF densities are assessed using PGP9.5 IHC. A) IHC of a control db+ foot pad. B) IHC of a db/db foot pad. Quantitation of foot pad densities presented as fiber number/mm of epidermis in C) the average reading ± standard error of the mean (SEM) and D) the individual animal measurements. d = dermis, e = epidermis, arrows = intraepidermal nerve fiber, arrowheads = dermal fiber bundles. [Methods in Neuropathy Manual online at www.amdcc.org.]

Advanced Neuropathy Phenotyping

At the request of the AMDCC investigator, the C57BLKS db/db animals underwent advanced neuropathy phenotyping. The components of advanced phenotyping were chosen by the investigator in consultation with the Neuropathy Phenotyping Core and included TUNEL staining, nitrotyrosine IHC and biochemical measurements of oxidative stress. TUNEL staining is used to identify cells containing fragmented DNA, an indicator of cellular injury. DRG neurons from db/db mice are strongly TUNEL positive when compared to neurons from db+ control animals (Fig. 3A and B). Positive IHC for nitrotyrosine (NT) indicates the presence of nitrosylated proteins, a downstream marker of oxidative stress (7). DRG neurons from db/db mice are strongly positive when compared to neurons from db+ control animals (Fig. 3C), confirmed by pixel quantitation of IHC fluorescence (Fig. 3D).

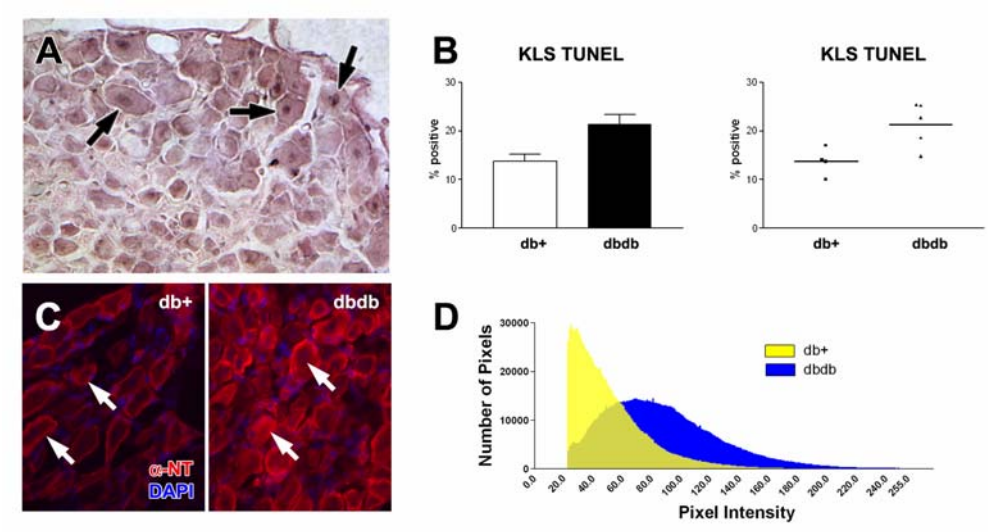

Fig. 3. Neuropathy Advanced Phenotyping: TUNEL and Nitrotyrosine IHC. A) TUNEL positive sensory neurons (arrows) were detected in the lumbar DRG of db/db mice at 24 weeks, B) Increased number of TUNEL labeled DRG in db/db mice at 24 weeks, $p < 0.05$. Five animals per group and > 150 neurons per animal were counted. Results are expressed as the percent TUNEL positive cells out of total neurons counted with the average reading ± SEM on the left and the individual animal measurements on the right, C) NT IHC reveals an increase in nitrosylated proteins within DRG neurons from db/db compared to db+ mice [nuclei stained with DAPI], D) Histograms of the fluorescence signal indicate a relative increase in the intensity of NT IHC in DRG from db+ versus db/db mice. [Methods in Neuropathy Manual online at www.amdcc.org]

Biochemical measurements of oxidative stress parallel the morphological markers of injury and are a means of quantitating DN severity (7). Db/db animals have increased DRG total reactive antioxidant potential (TRAP), sciatic nerve NADH oxidase and catalase, all indicating increased oxidative stress (Fig. 4 A to C)

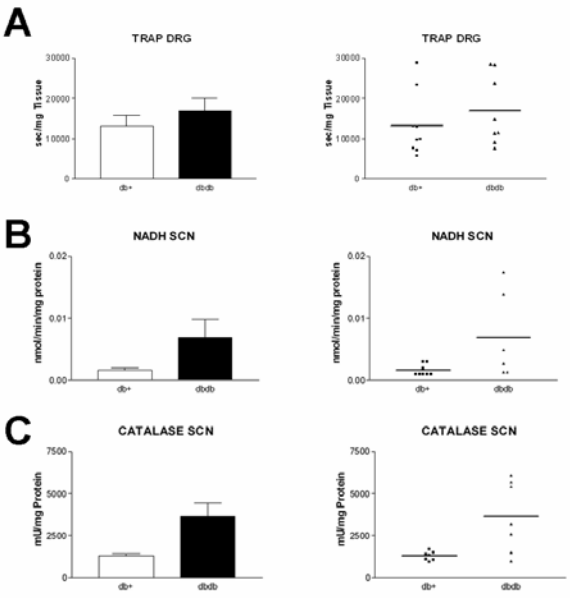

Fig. 4. Neuropathy Advanced Phenotyping: Biochemical Measurements of Oxidative Stress. A range of oxidative stress measures are used to assess nerve function in control (db+, open bars) versus diabetic (db/db, black bars) mice. In each lettered panel, the average reading ± SEM is presented on the left and the individual animal measurements on the right. Db/db mice have increased A) DRG total reactive antioxidant potential (TRAP), B) Sciatic nerve (SCN) NADH oxidase, and C) catalase, all markers of DN (7). [Methods in Neuropathy Manual online at www.amdcc.org]

In summary, the C57BLKS db/db mouse met all screening criteria for DN (Figs. 1 and 2), and underwent selected advanced phenotyping confirming oxidative injury to the nervous system (Figs. 3 and 4).

C57BLKS db/db mice ± resveratrol

Because of the presence of a clear DN phenotype, the C57BLKS db/db mice were selected for an intervention trial with the antioxidant resveratrol, administered for 12 weeks when the animals reached 8 weeks of age. While there were clear trends, there were no statistically significant changes in nerve function with resveratrol treatment between untreated and treated diabetic animals. This finding is

particularly interesting, given the fact that the high dose treatment arm had a decrease in glycated hemoglobin.

Table 2. Body weight, plasma glucose, glycated hemoglobin, plasma insulin level, total cholesterol and trigriceride in db/+ and db/db mice treated with/without resveratrol (RES)

Values are ± SEM, *p < 0.05 versus untreated db+ mice; †p < 0.05 versus untreated db/db mice; ‡p < 0.05 versus 10 mg/kg RES treated db/db mice.

Strain	Group	Body Weight (g)	Plasma glucose (mg/dl)	Glycated hemoglobin (%)
db/+	Untreated	26.0 ± 0.5	88.8 ± 3.8	5.1 ± 0.2
	10 mg/kg resveratrol	26.4 ± 0.6	81.8 ± 4.6	5.7 ± 0.2
	20 mg/kg resveratrol	27.4 ± 0.4	84.1 ± 3.0	5.9 ± 0.2
db/db	Untreated	45.7 ± 0.9*	325.8 ± 12.8*	10.5 ± 0.5*
	10 mg/kg resveratrol	45.4 ± 1.5*	313.7 ± 14.4*†	10.0 ± 0.4*
	20 mg/kg resveratrol	46.6 ± 1.1*	274.4 ± 19.6*†‡	9.1 ± 0.4*†

Table 3. Evaluation of peripheral nerve function in db/+ and db/db mice treated with/without RES Values are ± SEM, *p < 0.05 versus untreated db+ mice.

Strain	Group	Body Weight (g)	Glycated Hb (%)	Triglyceride (mg/dl)	SMNCV (m/sec)	TSNCV (m/sec)
db/+	Untreated	26.0 ± 0.5	5.1 ± 0.2	114.1 ± 10.3	23.4 ± 1.2	38.0 ± 1.1
	20 mg/kg res	27.4 ± 0.4	5.9 ± 0.2	122.6 ± 9.4	27.4 ± 0.4	37.4 ± 3.4
db/db	Untreated	45.7 ± 0.9*	10.5 ± 0.5*	169.9 ± 15.1*	16.9 ± 0.9*	26.0 ± 2.7*
	20 mg/kg res	46.6 ± 1.1*	9.1 ± 0.8*	161.9 ± 18.1*	15.1 ± 0.5*	22.8 ± 2.2*

GCLC+/- db/db mice and Glut1tg db/db. The γ-glutamate cysteine ligase (GCLC) heavy chain +/- mice are viable but show substantial decreases in GCLC protein and activity, and an approximately 20% decrease in glutathione levels. Thus, the GCLC +/- mouse should be a

useful genetic model for mild endogenous oxidative stress, which could be substantially increased in diabetes. In parallel, Glut 1 overexpression should increase glucose uptake and increase oxidative stress. Given the resistance of normal C57Bl/6J mice to STZ diabetes, we bred GCLC +/- and Glut1tg into the db/db C57BL/6J background resulting in 4 experimental groups for each gene: GCLC+/- db/db, GCLC+/+ db/db, GCLC+/- db/+, GCLC+/+ db/+ and Glut1 db/db, Glut1tg db/db, Glut1 db/+, Glut1tg db/+ Mice were fed breeder chow. At 24 weeks, there are the expected differences in behavioral tests and conduction velocities between the diabetic and control mice of each genotype but no significant difference between the GCLC+/+ dbdb and GCLC+/- dbdb mice (Fig. 5) or the Glut1tg dbdb and Glut1 dbdb animals (Fig. 6).

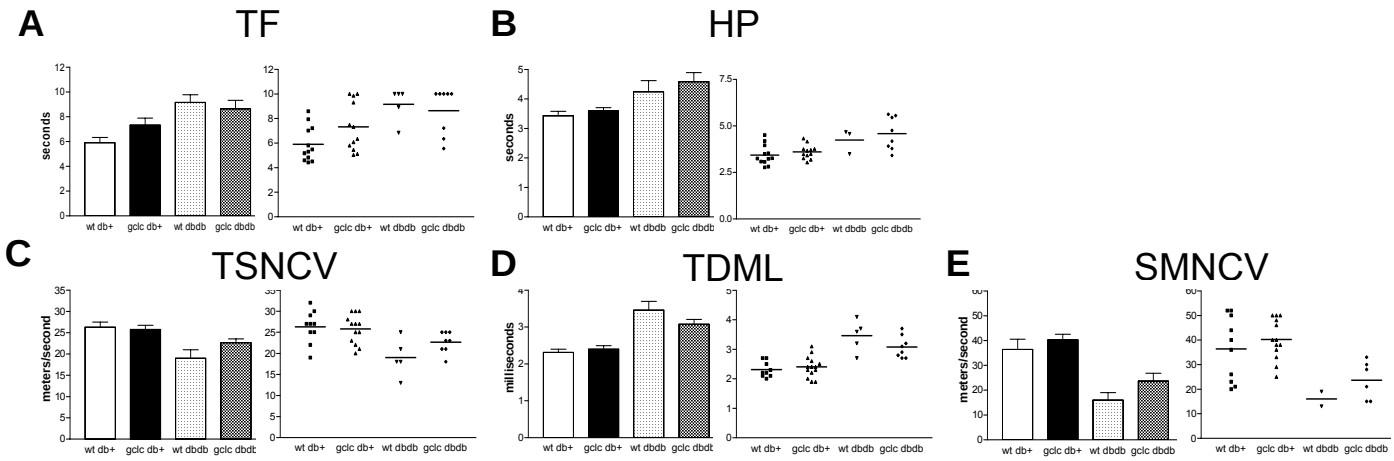

Fig. 5. Nerve conduction velocities and sensory measures in GCLC+/+ and +/- Db mice. Panels A-E illustrate changes in nerve function and physiology in the GCLC+/+ and +/- dbdb and db+ mice following 24 weeks of diabetes. A) Tail Flick (TF) latency, B) Hind Paw (HP) latency, C) Tail sensory nerve conduction velocity (TSNCV), D Tail distal motor latency (TDML), E) Sciatic motor nerve conduction velocity (SMNCV),

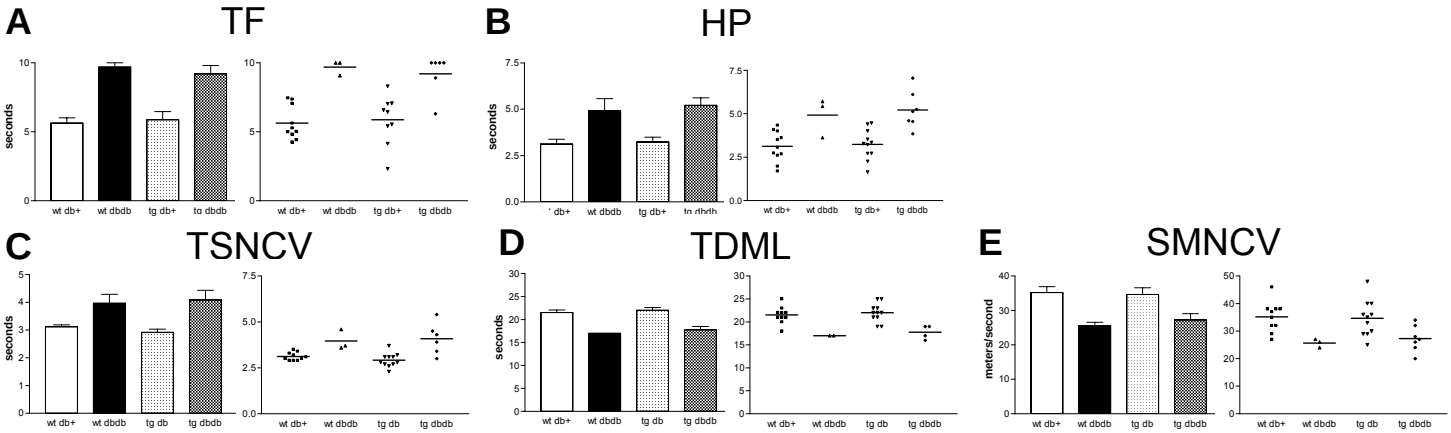

Fig. 6. Nerve conduction velocities and sensory measures in Glut1 wildtype and transgenic (tg) and +/- Db mice. Panels A-E illustrate changes in nerve function and physiology in the glut1 and glut1tg and +/- dbdb and db+ mice following 24 weeks of diabetes. A) Tail Flick (TF) latency, B) Hind Paw (HP) latency, C) Tail sensory nerve conduction velocity (TSNCV), D Tail distal motor latency (TDML), E) Sciatic motor nerve conduction velocity (SMNCV),

Targeted Disruption of SOD2

We have used the SOD2+/- mouse to examine whether a predisposition to increased oxidative stress would increase the severity of DN. STZ treatment of male C57Bl6 SOD2+/+ and +/- mice resulted in increased levels of blood glucose and glycated hemoglobin but these animals did not develop DN over the course of 6 months. In the genetic model of type 2 diabetes, the C57Bl6 db/db, SOD2+/+ and +/- animals became hyperglycemic at 4 weeks of age. Hyperglycemia and weight gain were not influenced by the SOD2 genotype. As we have previously reported, there was evidence of an increased neuropathic phenotype in the heterozygote animals on the dbdb background compared to the dbdb animals alone after 24 weeks. These encouraging data lead us to pursue targeted disruption of SOD2 using Cre-recombinase with the nestin promoter and floxed $SOD^{-/-}$. Initial data comparing diabetic C57Bl/6J flox/flox (no targeted disruption of SOD2) with diabetic C57Bl/6J Cre flox/flox (targeted disruption of SOD2) suggest that disruption of SOD2 in neurons results in a more pronounced neuropathy phenotype. Both models are hyperglycemic with STZ-induced diabetes. After 16 weeks of diabetes, glycated hemoglobin levels are elevated in both diabetic C57Bl/6J flox/flox (no targeted disruption of SOD2) and diabetic C57Bl/6J Cre flox/flox (targeted disruption of SOD2). (Fig. 7A). Both the tail flick and hind paw latencies are increased in both animals, reflecting loss of thermal sensation (Fig. 7B and C). Tail distal motor latencies are increased (Fig. 7E) while tail sensory and sciatic motor conduction velocities are decreased in both conditions (Fig. 7D and F), a pattern confirming DN. In each neurophysiological measurement, the diabetic cre flox/flox (targeted disruption of SOD2) mice have values compatible with a more severe neuropathic phenotype when compared to the diabetic flox/flox (no targeted disruption of SOD2) mice, and this is after only 16 weeks of diabetes.

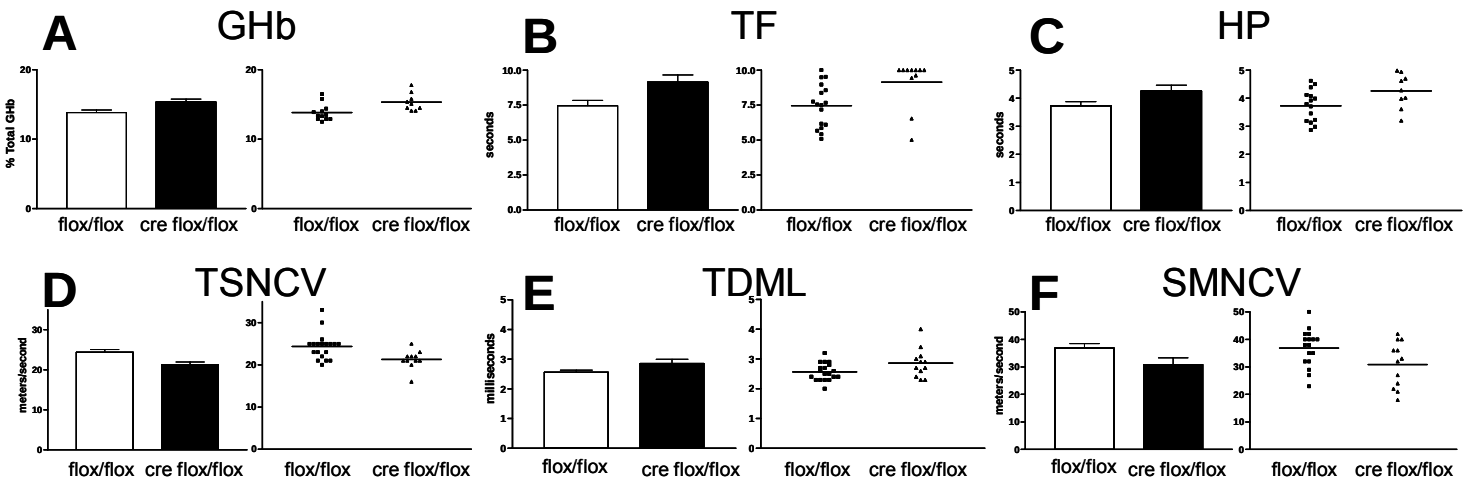

Figure 7. Neuropathy Phenotyping Using Clinical and Electrophysiological Assessments. A full range of neuropathy phenotyping measures are used to assess nerve function in diabetic C57Bl/6J flox/flox (no targeted disruption of SOD2, open bars) versus diabetic C57Bl/6J Cre flox/flox (targeted disruption of SOD2, black bars) mice. In each lettered panel, the average reading ± standard error of the mean (SEM) is presented on the left and the individual animal measurements on the right. A) Both mice have increased glycated hemoglobin (GHb), B) Tail flick latency (TF) and C) Hind paw latencies (HP) are increased in both mice, D) Tail sensory nerve conduction velocity (TSNCV) is decreased in both mice, E) Tail distal motor latency (TDML) is increased in both mice, and F) Sciatic motor nerve conduction velocity (SMNCV) is decreased in both mice.

Further support for an increased neuropathic phenotype is shown by advanced neuropathy phenotyping. There is increased anatomical evidence of nerve fiber loss in diabetic C57Bl/6J Cre flox/flox mice when compared to diabetic C57Bl/6J flox/flox. The hind paws of control mice are normally innervated with a full component of PGP9.5 immunoreactive fibers (typically around 40 fibers per mm of tissue, data not shown) while both diabetic C57Bl/6J Cre flox/flox and diabetic C57Bl/6J flox/flox mice have nerve fiber loss and decreased intraepidermal nerve fiber densities (IENF) (Fig. 8). The diabetic Cre flox/flox (targeted disruption of SOD2) mice have a more severe loss of IENF when compared to the diabetic flox/flox (no targeted disruption of SOD2) mice after only 16 weeks of diabetes.

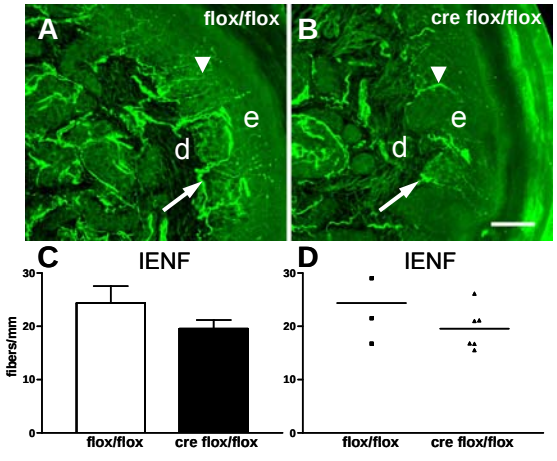

Figure 8. Neuropathy Phenotyping Using Morphological Techniques. IENF densities are assessed using PGP9.5 immunohistochemistry (IHC). A) IHC of a flox/flox foot pad. B) IHC of a cre flox/flox foot pad. C) Quantitation of foot pad densities presented as fiber number/mm of epidermis. D) Individual animal measurements. Arrowheads = intraepidermal nerve fibers, arrows = dermal fiber bundles. e = epidermis, d = dermis

Continued advanced phenotyping revealed that diabetic mice with targeted disruption of SOD2 demonstrate elevated oxidative stress

compared to diabetic mice with non-disrupted SOD2 expression. We observed evidence of increased oxidative stress in DRG neurons from the diabetic C57Bl/6J Cre flox/flox mice compared to the diabetic C57Bl/6J flox/flox mice. Measures of oxidative injury are indicators of DN. These include TUNEL staining and nitrotyrosine immunohistochemistry (IHC). TUNEL staining is used to identify cells containing fragmented DNA, an indicator of cellular injury. DRG neurons from the diabetic C57Bl/6J flox/flox and diabetic C57Bl/6J Cre flox/flox mice are TUNEL positive (Fig. 9A and B), with more TUNEL positive DRG in the Cre flox/flox animals. Positive IHC for nitrotyrosine (NT) indicates the presence of nitrosylated proteins, a downstream marker of oxidative stress in DN. DRG neurons from the diabetic C57Bl/6J flox/flox and diabetic C57Bl/6J Cre flox/flox mice are positive when compared to nondiabetic mice (Fig. 9C), confirmed by pixel quantitation of IHC fluorescence (Fig. 9D). Again, mice with the targeted disruption in neurons of SOD2 (C57Bl/6J Cre flox/flox) have a greater degree of NT IHC compared to mice with the normal full expression of SOD2 in neurons (C57Bl/6J flox/flox),

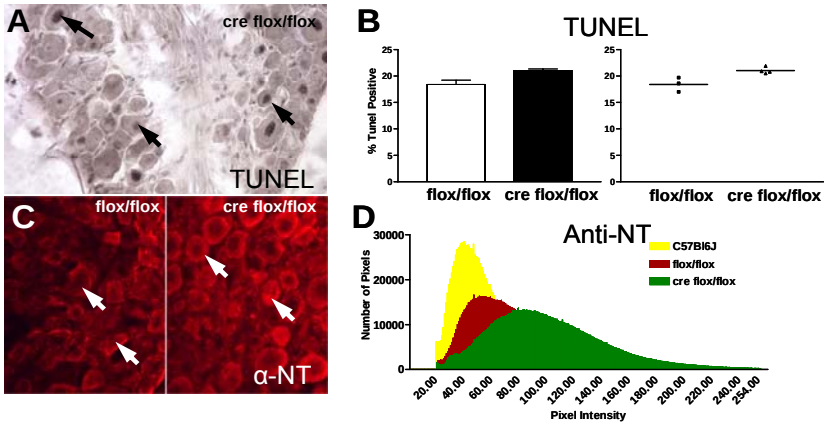

Figure 9. TUNEL and Nitrotyrosine IHC. A) TUNEL positive sensory neurons (arrows) are detected in the lumbar DRG of C57Bl/6J Cre flox/flox mice at 24 weeks, B) An increase in TUNEL positive DRG are detected in Cre flox/flox mice. 3-4 animals per group and > 150 neurons per animal are counted. Results are expressed as the percent TUNEL positive cells out of total neurons counted with the average reading ± SEM on the left and the individual animal measurements on the right, C) Nitrotyrosine (NT) IHC reveals an increase in nitrosylated proteins within DRG neurons from cre flox/flox (right) compared to flox/flox (left) mice, D) Histograms of the fluorescence signal indicate a relative increase in the intensity of NT IHC in DRG from cre flox/flox versus flox/flox mice.

Akita mice ± rosiglitazone

In a continuing attempt to discover improved models of murine DN, we phenotyped the Akita mouse after 24 weeks of STZ diabetes. A small group of animals were also treated with rosiglitazone (see Dr. Brosius's report) and underwent focused phenotyping. Despite hyperglycemia (see Dr. Brosius's report), there was a trend toward the development of DN as measured by increased tail flick and hind paw latencies (Fig. 10 A and B) but no differences in conduction velocities (Fig. 10 C-E) or IENF (Fig. 10F). Rosiglitazone did not ameliorate the effects on sensory latencies (Fig. 11).

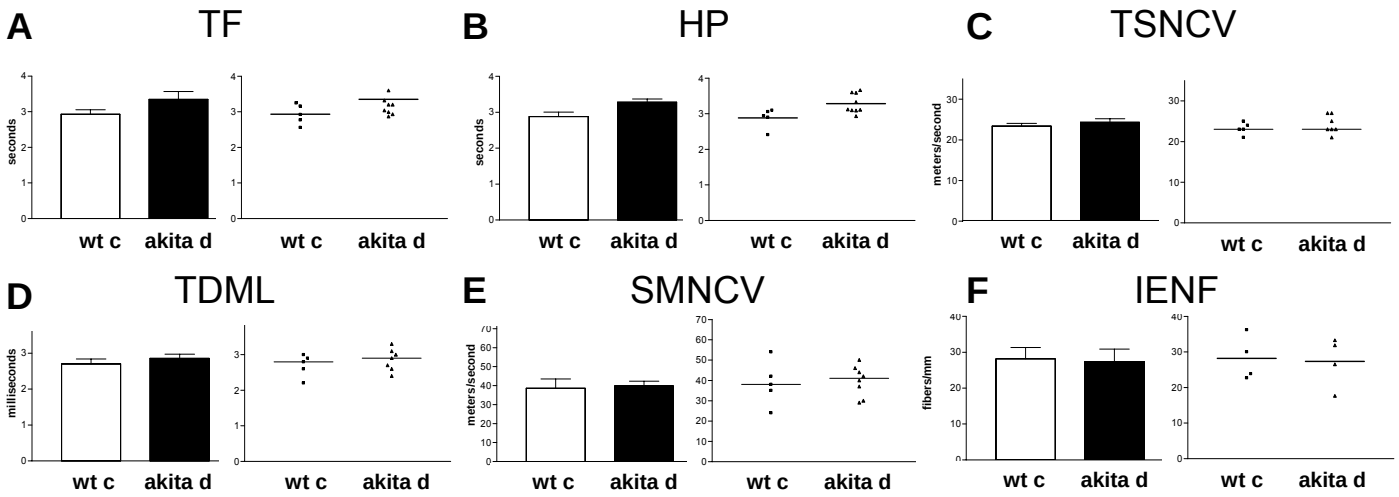

Fig.10 Nerve conduction velocities and sensory measures in Akita mice. Panels A-E illustrate changes in nerve function and physiology in the nondiabetic Akita (wt c) and the Akita mouse after 24 weeks of STZ diabetes (akita C) A) Tail Flick (TF) latency, B) Hind Paw (HP) latency, C) Tail sensory nerve conduction velocity (TSNCV), D Tail distal motor latency (TDML), E) Sciatic motor nerve conduction velocity (SMNCV), F) Intraepidermal nerve fiber density (IENF).

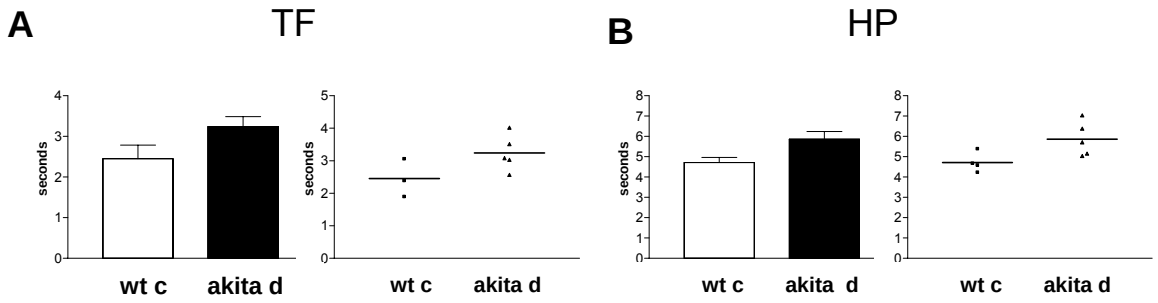

Fig.11 Sensory measures in Akita mice + rosiglitazone. Panels A and B illustrate changes in nerve function in the nondiabetic Akita (wt c) and the STZ diabetic Akita mouse. Both groups of animals were treated with rosiglitazone s (akita C). A) Tail Flick (TF) latency, B) Hind Paw (HP) latency.

2. Collaboration with your Group:

The Neuropathy Phenotyping Core has been an integral part in developing new mouse models of DN as part of the grant to Dr. Brosius. Rodent models of diabetes fail to develop changes that closely resemble human diabetic nephropathy or neuropathy. While the reasons for the resistance of rodents to full-blown complications are likely multiple, they may include an increased resistance to oxidative stress or the absence of important genetic susceptibility genes (5;17). Our general strategic approach to this dilemma is to accelerate the injury of diabetes by predisposing critical cells within the peripheral nervous system to glucose-mediated oxidative injury. Our ongoing work with Dr. Brosius is outlined in Table 1.

Finally, as described in Dr. Brosius' report, interactions between the nephrology and neuropathy investigators at Michigan occur almost daily. Coordination of nephropathy and neuropathy phenotyping begins with the birth of the animals and continues through their assignment to an experimental group to final tissue collection.

3. Collaborations With Other AMDCC Groups:

Three AMDCC groups actively used the Neuropathy Phenotyping Core: the Rockefeller University (Dr. Breslow), University of North Carolina, Chapel Hill (Drs. Clemmons and Nichol) and Cleveland Clinic (Dr. Danshgari). We also anticipate receiving animals from Dr. Breyer at Vanderbilt. These collaborations are presented in Table 4.

Table 4. Animal Models: Ongoing Neuropathy Phenotyping for AMDCC Investigators outside of U of M

LDLRO mice	C57BL/6J	Phenotyping complete	2/05
Pdx mice	C57BL/6J	Phenotyping complete	4/05
pig		Phenotyping attempted x 3	

Dr. Breslow's group from the Rockefeller University sent over 30 samples for IEFD analysis from the ob/ob LDLR0 and control LDLR0 mice. The feet were shipped in 4% paraformaldehyde and upon arrival were dissected, cryoprotected, embedded and sectioned. Immunohistochemistry for PGP9.5 confirms the presence of epidermal fibers. There was no difference in the IEFD between the two groups, although technical difficulties were encountered with fixation. In addition to the foot pads, 2 year old pdx+/+ and pdx+/- mice were sent for neuropathy phenotyping. These animals were examined for nerve function according to our established protocols. There was a statistically significant increase in tail flick latency and decrease in the sciatic motor nerve conduction velocity in the pdx+/- mice when compared to the pdx+/+ (Fig. 12). The eyes were placed in 10% formalin and shipped to Dr. Kern and the bladders were cryoembedded for sectioning for Dr. Danshgari. Kidneys were given to the Brosius laboratory here at Michigan.

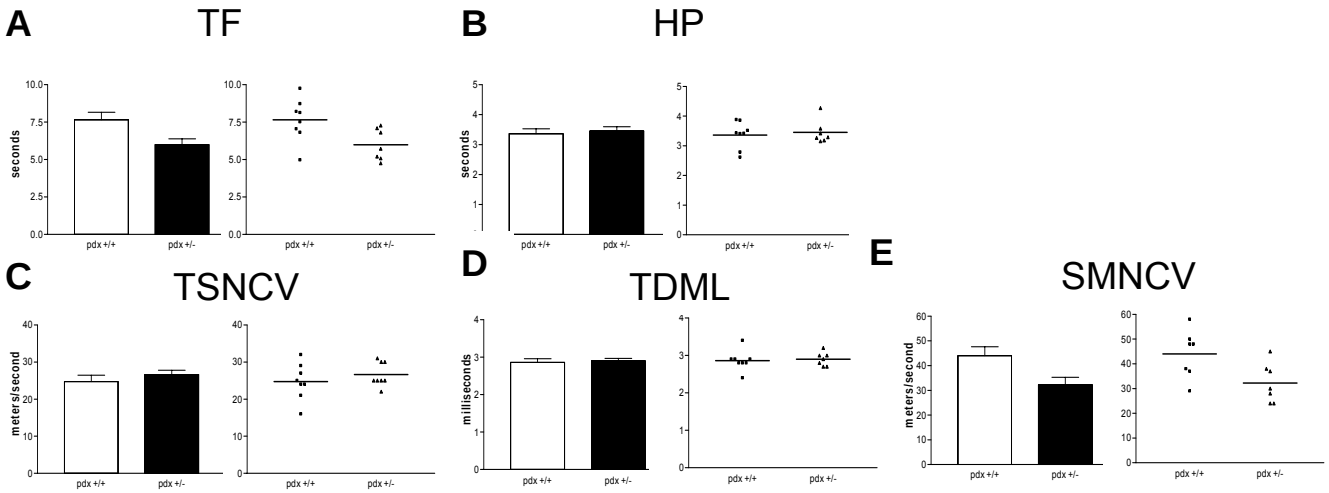

Fig.12 Nerve conduction velocities and sensory measures in pdx+/+ and pdx+/- mice. Panels A-E illustrate changes in nerve function and physiology in the pdx+/+ and pdx+/- mice 2 years of age A) Tail Flick (TF) latency, B) Hind Paw (HP) latency, C) Tail sensory nerve conduction velocity (TSNCV), D Tail distal motor latency (TDML), E) Sciatic motor nerve conduction velocity (SMNCV).

Technical difficulties have been encountered in the analysis of IEFD in the pig skin sent by Drs. Clemmons and Nichol. Due to the amount of subdermal fat, pig skin sections did not stay on the slides through the entire IHC procedure. We examined the skin under two different protocols. The first was sent to us by Dr. Andrew Mizisin University of California San Diego (UCSD) (via the helpful intervention and guidance of Dr. Calcutt, UCSD). Biopsy punches of the skin were taken and 80% of the fat was removed and the samples underwent paraffin embedding and sectioning (4 µm). IHC of these samples was unsuccessful. It may be that paraffin embedding is not compatible with PGP9.5 antibody cross reactivity in pig. We also examined 20 µm cryosections of re-biopsied, fat trimmed pig skin but again encountered the technical difficulties of tissue adherence onto slides.

We have continued to work with Dr. Firouz Danshgari who has brought his staff to the Neuropathy Phenotyping Core to measure bladder elasticity of selected animal models. Dr. Danshgari and his staff have established the feasibility of performing this test on a recovery basis and that this technique is an important addition to overall model characterization. We also continue to send eyes to Dr. Timothy Kern. This collaboration lead to an application to form a Mouse Metabolic Phenotyping Center between University of Michigan (Feldman and Brosius), Cleveland Clinic (Danshgari) and Case Western (Kern).

4. Pertinent non-AMDCC Collaborations:

Listed below are the major collaborative projects related to the consortium goals but independent of AMDCC:

1. We have obtained IRS -/- mice from Dr. at the Joslin Clinic and the SOD1-/- mice from Dr. John Faulkner at the University of Michigan. In both instances, these mice are 2 years old. Our plan is to phenotype these animals within the next 3 months.
2. Dr. Feldman is the Principal Investigator for several collaborative NIH grants investigating the etiology, pathogenesis and treatment of diabetic polyneuropathy. .
3. Dr. Feldman is an investigator in neuropathy aspects of the multi-institutional Epidemiology of Diabetes Interventions and Complications (EDIC) study.

5. Address previous EAC Comments:

Please see Dr. Coffman's report.

Reference List

(1) Feldman EL, Stevens MJ, Russell JW, Greene DA. Diabetic neuropathy. In: Taylor S, editor. Current Review of Diabetes. Current Medicine; 1999. p. 71-83.

(2) Windebank AJ, Feldman EL. Diabetes and the nervous system. In: Aminoff MJ, editor. Neurology and General Medicine. 3rd ed. Churchill Livingstone; 2001. p. 341-64.

(3) Feldman EL, Stevens MJ, Russell JW, Greene DA. Diabetic neuropathy. In: Becker KL, editor. Principles and Practice of Endocrinology and Metabolism. 3rd ed. Philadelphia: Lippincott Williams & Wilkins; 2001. p. 1391-9.

(4) Feldman EL, Stevens MJ, Russell JW, Greene DA. Somatosensory neuropathy. In: Porte D, Jr., Sherwin RS, Baron A, editors. Ellenberg and Rifkin's Diabetes Mellitus. 6th ed. McGraw Hill; 2002. p. 771-88.
(5) Feldman EL. Oxidative stress and diabetic neuropathy: a new understanding of an old problem. J Clin Invest 2003 Feb;111:431-3.
(6) Vincent AM, Feldman EL. New insights into the mechanisms of diabetic neuropathy. Reviews in Endocrine & Metabolic Disorders 2004;5:227-36.
(7) Vincent AM, Russell JW, Low P, Feldman EL. Oxidative stress in the pathogenesis of diabetic neuropathy. Endocr Rev 2004;25:612-28.
(8) Boulton AJ, Vinik AI, Arezzo JC, Bril V, Feldman EL, Freeman R, et al. Diabetic neuropathies: a statement by the American Diabetes Association. Diabetes Care 2005 Apr;28:956-62.
(9) Sullivan KA, Feldman EL. New developments in diabetic neuropathy. Curr Opin Neurol 2005 Oct;18:586-90.
(10) Sima AAF, Shafrif E. Animal Models in Diabetes: A Primer. Amsterdam: Taylor and Francis; 2000.
(11) Chua SC, Jr., Chung WK, Wu-Peng XS, Zhang Y, Liu SM, Tartaglia L, et al. Phenotypes of mouse diabetes and rat fatty due to mutations in the OB (leptin) receptor. Science 1996 Feb 16;271:994-6.
(12) Hummel KP, Dickie MM, Coleman DL. Diabetes, a new mutation in the mouse. Science 1966 Sep 2;153:1127-8.
(13) Chen H, Charlat O, Tartaglia LA, Woolf EA, Weng X, Ellis SJ, et al. Evidence that the diabetes gene encodes the leptin receptor: identification of a mutation in the leptin receptor gene in db/db mice. Cell 1996 Feb 9;84:491-5.
(14) Arezzo JC. New developments in the diagnosis of diabetic neuropathy. Am J Med 1999 Aug 30;107:9S-16S.
(15) Kennedy WR, Wendelschafer-Crabb G, Johnson T. Quantitation of epidermal nerves in diabetic neuropathy. Neurology 1996;47:1042-8.
(16) Christianson JA, Riekhof JT, Wright DE. Restorative effects of neurotrophin treatment on diabetes-induced cutaneous axon loss in mice. Exp Neurol 2003 Feb;179:188-99.
(17) Greene DA, Obrosova I, Stevens MJ, Feldman EL. Pathways of glucose-mediated oxidative stress in diabetic neuropathy. In: Packer L, Rosen P, Tritschler HJ, King GL, Azzi A, editors. Antioxidants in diabetes management.New York: Marcel Dekker; 2000. p. 111-9.